10084 *Inorg. Chem.* **2009**, *48*, 10084–10092
DOI: 10.1021/ic9010604

Inorganic Chemistry
Article

Redox Effects on the Coordination Geometry and Heme Conformation of Bis(*N*-methylimidazole) Complexes of Superstructured Fe-Porphyrins. A Spectroscopic Study

Carole Le Moigne,[†] Thierry Picaud,[†] Alain Boussac,[†] Bernard Loock,[‡] Michel Momenteau,[‡,§] and Alain Desbois*[,†]

[†]*Service de Bioénergétique, Biologie Structurale et Mécanismes (SB²SM) et URA CNRS 2096, Institut de Biologie et Technologie de Saclay (iBiTec-S), CEA/Saclay, F-91191 Gif-sur-Yvette Cedex, France, and* [‡]*Institut Curie, Centre Universitaire, F-91405 Orsay Cedex, France.* [§]*Deceased.*

Received June 2, 2009

Electronic absorption, electron paramagnetic resonance (EPR), and Soret-excited resonance Raman (RR) spectra are reported for bis(*N*-alkylimidazole) complexes of various iron(III)-"basket-handle" (Fe(III)BHP^+) and "picket-fence" (Fe(III)PFP^+) porphyrins in methylene chloride. The Fe(III)BHP^+ derivatives consist of four cross-trans (CT) and two adjacent-cis (AC) -linked in which the composition and the length of the handles are variable (CT Fe(III)$[(C_{11}Im)_2^+]$, CT and AC Fe(III)$[((C_4)_2\phi)_2]^+$, CT Fe(III)$[((C_3)_2\phi)(C_{12})]^+$, CT and AC Fe(III)$[((C_3)_2\phi)_2]^+$). The meso-$\alpha\alpha\beta\beta$ and meso-$\alpha\beta\alpha\beta$ atropisomers of Fe(III)-tetrakis(o-pivalamidophenyl)-porphyrins represents the Fe(III)PFP^+ derivatives (Fe(III)$\alpha\alpha\beta\beta$-$T_{piv}PP^+$ and Fe(III)$\alpha\beta\alpha\beta$-$T_{piv}PP^+$, respectively). The absorption and RR data obtained for these ferric compounds were compared to those previously published for the homologous ferrous complexes (Picaud, T.; Le Moigne, C.; Loock, B.; Momenteau, M.; Desbois, A. *J. Am. Chem. Soc.* **2003**, *125*, 11616 and Le Moigne, C.; Picaud, T.; Boussac, A.; Loock, B.; Momenteau, M.; Desbois, A. *Inorg. Chem.* **2003**, *42*, 6081). The Soret band position of the eight investigated ferric compounds is observed between 417 and 424 nm, indicating that none of the complexes possesses a planar heme. The EPR spectra show that most of the Fe(III)BHP^+ complexes and all the Fe(III)PFP^+ complexes are rhombic B-type hemichromes (g_{max} = 2.86−2.96). Notable exceptions concern the bis(*N*-methylimidazole) complexes of two CT Fe(III)BHP^+. The Fe(III)BHP^+ with the shortest handles (Fe(III)$[((C_3)_2\phi)_2]^+$) exhibits a *g* value at 2.80. When the handles are lengthened by two methylene units (Fe(III)$[((C_3)_2\phi)_2]^+$), the EPR spectrum corresponds to a mixture of two "highly anisotropic low-spin " or "large g_{max}" type I EPR signals, a major species at *g* = 3.17 and a minor species at *g* = 3.77. All these EPR data were converted in terms of dihedral angle formed by the rings of the axial ligands. The RR spectra of the Fe(III)BHP^+ and Fe(III)PFP^+ complexes exhibited variable frequencies for the structure-sensitive ν_2 and ν_8 lines (1558−1563 cm^{-1} and 386−401 cm^{-1}, respectively). In considering the ability of the different superstructures to stabilize particular out-of-plane distortions, this vibrational information was analyzed in terms of heme structure through changes in core size and Fe−N(pyrrole) bond length, in relation to changes in coordination geometry. The bis(*N*-methylimidazole) complex of Fe(III)$[((C_3)_2\phi)_2]^+$ was found to be the most distorted with a strongly ruffled tetrapyrrole. Because of a handle asymmetry, the heme conformation of the bis(*N*-methylimidazole) complex of Fe(III)$[((C_3)_2\phi)(C_{12})]^+$ was deduced to be a composition of ruffled and domed structures. The heme structure of the other complexes is a mixture of ruffled and saddled or ruffled and waved conformations. Taking into account our previous data on the ferrous series, this investigation provides information about the reorganization of the heme structure upon iron oxidation. The general trend is a decrease of either the core-size, or the Fe-N(pyrrole) bond length, or both. However, we demonstrated that the heme superstructures precisely control the nature and the extent of the tetrapyrrole reshaping. These results point out similar possible effect in the heme proteins, considering both an analogy between porphyrin superstructures and amino acids forming the heme sites and the diversity of the heme environments in the proteins.

Introduction

Iron-hemes axially coordinated by two histidine ligands are the active sites of many biological systems. The most known are cytochrome b_5, cytochrome b_{559}, flavocytochrome b_2, tetraheme cytochrome c_3, neuroglobin, the b-type hemes of cytochrome bc_1 and b_6f complexes, heme b of sulfite oxidase, and heme a of cytochrome oxidase. Because of variations in packing of the amino acid residues in the heme pockets, the H-bonding states of the imidazole N−H protons

*To whom correspondence should be addressed. E-mail: alain.desbois@cea.fr. Phone: 33 (0)1 69 08 37 22. Fax: 33 (0)1 69 08 91 11.

 Published on Web 10/09/2009

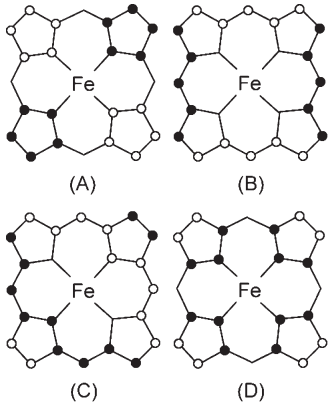

Figure 1. Schematic representation of saddled (A), ruffled (B), waved (C), and domed (D) conformations. The filled and open circles indicate displacements of the C or N atoms above and below the mean porphyrin plane, respectively.

to protein residues, the conformation of the porphyrin tetrapyrrole and the relative and absolute orientations of the imidazole planes with respect to the Fe−N(pyrrole) bonds are structural parameters that can affect the redox, biological, and spectroscopic properties of the hemes.[1]

A number of heme model compounds has been synthetized to simulate the coordination sites of these natural bis-(histidine) Fe-heme complexes. Structural characterizations of these complexes clearly distinguish the Fe(II)- and Fe(III)-porphyrinate complexes. On the one hand, a series of imidazole-ligated Fe(III) compounds in which the imidazoles are unhindered show the ligand rings more or less rotated with respect to the $Fe-N_4$(pyrrole) axes and a ruffled porphyrin (Figure 1).[2] On the other hand, homologous bis(imidazole) complexes of Fe(II)-porphyrins exhibit a planar porphyrin macrocycle and parallel orientations for the two axial ligand rings.[3]

Previous spectroscopic investigations on bis(*N*-methylimidazole) (bis(*N*-MeIm)[4] complexes of "superstructured" Fe(II)-porphyrins have shown that basket-handle Fe(II)-porphyrins (BHP) can adopt a ruffled conformation when the strain exerted by the handles is sufficiently strong.[5] The effects of the iron oxidation on simple Fe-porphyrins is to decrease the lengths of the axial Fe−N(imidazole) and equatorial Fe−N(porphyrin) bonds, generating a porphyrin

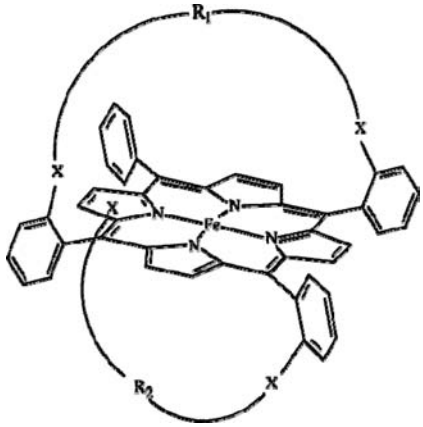

Figure 2. Schematic structure of the cross-trans-linked iron(III)-"basket-handle" porphyrins used in this study.

Table 1. Molecular Structures of the Cross-Trans-Linked Fe(III)-Basket-Handle Porphyrins Studied in This Work

FeBHP	X	R_1	R_2
$Fe[(C_{11}Im)_2]$	NH	CO-$(CH_2)_4$-CH(Im)-$(CH_2)_4$-CO	CO-$(CH_2)_4$-CH(Im)-$(CH_2)_4$-CO
$Fe[((C_4)_2\phi)_2]$	O	$(CH_2)_4$-C_6H_4-$(CH_2)_4$	$(CH_2)_4$-C_6H_4-$(CH_2)_4$
$Fe[((C_3)_2\phi)(C_{12})]$	NH	CO-$(CH_2)_2$−C_6H_4-$(CH_2)_2$−CO	CO-$(CH_2)_{10}$-CO
$Fe[((C_3)_2\phi)_2]$	O	$(CH_2)_3$-C_6H_4-$(CH_2)_3$	$(CH_2)_3$-C_6H_4-$(CH_2)_3$

ruffling and a rotation of the imidazole rings. A question presently concerns the behavior of Fe-porphyrin complexes having their heme already distorted under the reduced state. In other words, to which extent the redox state of the heme induces or not the porphyrin deformation? To answer to this question, we have investigated the bis(*N*-MeIm) complexes of Fe(III)BHP^+ and picket-fence Fe(III)-porphyrins (Fe(III)PFP^+) using absorption, EPR and resonance Raman (RR) spectroscopies.

Experimental Section

Four bis(*N*-MeIm) complexes of cross-*trans*-linked (CT) Fe(III)BHP^+ were studied, that is, the amide-linked 5,15:10,20-bis(2,2'-(5-imidazol-1-yl nonane-1,9-diamido)diphenyl)porphyrin ($Fe[(C_{11}Im)_2]$) and α-5,15-[2,2′-(dodecanediamido)diphenyl]-*β*-10,20-[2,2'(3,3′-(p-phenylene) dipropionamido)-diphenyl]porphyrin ($Fe(III)[((C_3)_2\phi)(C_{12})]^+$), and the ether-linked 5,15:10,20-bis(2,2'-[3,3′-(p-phenylene)dibutoxy]diphenyl)porphyrin ($Fe(III)[((C_4)_2\phi)_2]^+$) and 5,15:10,20-bis(2,2'-[3,3′-(p-phenylene)dipropoxy]diphenyl)porphyrin ($Fe(III)[((C_3)_2\phi)_2]^+$) (Figure 2, Table 1). To measure the influence of the insertion mode of the handles on the porphyrin structure, the bis(*N*-MeIm) complexes of the adjacent-cis (AC) isomers of Fe(III)$[((C_4)_2\phi)_2]^+$ and Fe(III)$[((C_3)_2\phi)_2]^+$ were also investigated.

(1) Shelnutt, J. A.; Song, X.-Z.; Ma, J.-G.; Jia, S.-L.; Jentzen, W.; Medforth, C. J. *Chem. Soc. Rev.* **1998**, *27*, 31.

(2) (a) Collins, D. M.; Countryman, R.; Hoard, J. L. *J. Am. Chem. Soc.* **1972**, *94*, 2066. (b) Little, R. G.; Dymock, K. R.; Ibers, J. A. *J. Am. Chem. Soc.* **1975**, *97*, 4532. (c) Scheidt, W. R.; Osvath, S. R.; Lee, Y. J. *J. Am. Chem. Soc.* **1987**, *109*, 1958. (d) Quinn, R.; Valentine, J. S.; Byrn, M. P.; Strouse, C. E. *J. Am. Chem. Soc.* **1987**, *109*, 3301. (e) Higgins, T.; Safo, M. K.; Scheidt, W. R. *Inorg. Chim. Acta* **1990**, *178*, 261. (f) Safo, M. K.; Gupta, G. P.; Walker, F. A.; Scheidt, W. R. *J. Am. Chem. Soc.* **1991**, *113*, 5497. (g) Silver, J.; Marsh, P. J.; Symons, M. C. R.; Svistunenko, D. A.; Frampton, C. S.; Fern, G. R. *Inorg. Chem.* **2000**, *39*, 2874.

(3) (a) Steffen, W. L.; Chun, H. K.; Hoard, J. L.; Reed, C. A. Abstract of Papers. 175th National Meeting of the American Chemical Society, Anaheim, CA; March 13, 1978; American Chemical Society: Washington, D.C., 1978; INOR 15. (b) Safo, M. K.; Scheidt, W. R.; Gupta, G. P. *Inorg. Chem.* **1990**, *29*, 626.

(4) Abbreviations used: *N*-MeIm, *N*-methylimidazole; LS: low-spin; TPP, tetraphenylporphyrinate; PFP, "picket-fence" porphyrinates; BHP, "basket-handle" porphyrinates; CT, cross-trans; AC, adjacent-cis; oop, out-of-plane; RR, resonance Raman, EPR, electronic paramagnetic resonance

(5) (a) Picaud, T.; Le Moigne, C.; Loock, B.; Momenteau, M.; Desbois, A. *J. Am. Chem. Soc.* **2003**, *125*, 11616. (b) Le Moigne, C.; Picaud, T.; Boussac, A.; Loock, B.; Momenteau, M.; Desbois, A. *Inorg. Chem.* **2003**, *42*, 6081.

(6) (a) Momenteau, M.; Mispelter, J.; Loock, B.; Bisagni, E. *J. Chem. Soc., Perkin Trans. I* **1983**, 189. (b) Schaeffer, C.; Momenteau, M.; Mispelter, J.; Loock, B.; Huel, C.; Lhoste, J.-M. *Inorg. Chem.* **1986**, *25*, 4577. (c) Momenteau, M.; J.; Loock, B.; Huel, C.; Lhoste, J.-M. *J. Chem. Soc., Perkin Trans. I* **1988**, 283.

(7) (a) Walker, F. A.; Buehler, J.; West, J. T.; Hinds, J. L. *J. Am. Chem. Soc.* **1983**, *105*, 6923. (b) Odo, J.; Imai, H.; Kyuno, E.; Nakamoto, K. *J. Am. Chem. Soc.* **1988**, *110*, 742. (c) Collman, J. P.; Gagne, R. R.; Halbert, T. R.; Marchon, J. C.; Reed, C. A. *J. Am. Chem. Soc.* **1973**, *95*, 7868. (d) Collman, J. P.; Gagne, R. R.; Reed, C. A.; Halbert, T. R.; Lang, G.; Robinson, W. T. *J. Am. Chem. Soc.* **1975**, *97*, 1427.

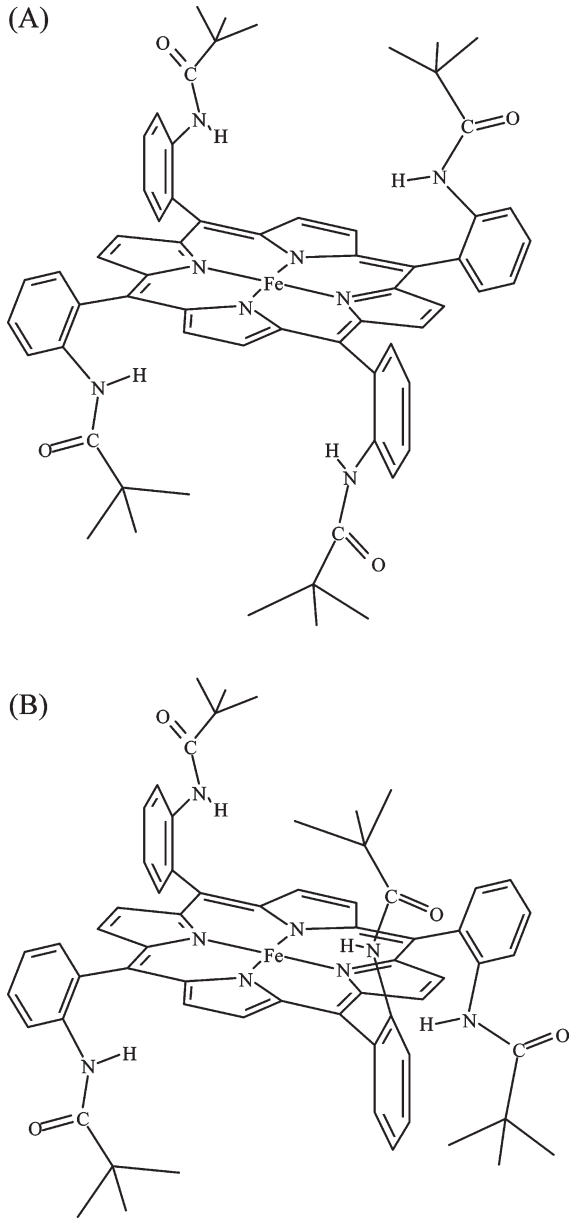

Figure 3. Schematic structures of the $\alpha\alpha\beta\beta$ (A) and $\alpha\beta\alpha\beta$ (B) atropisomers of Fe(III)-tetrakis(*o*-pivalamidophenyl)porphyrin.

As far as the Fe(III)PFP$^+$ compounds are concerned, the bis(base) complexes of the $\alpha\alpha\beta\beta$ and $\alpha\beta\alpha\beta$ atropisomers have been studied (Figure 3). The syntheses, purifications, characterizations, and structures of the Fe(III)BHP$^+$ and Fe(III)PFP$^+$ used in this study have been previously reported.[6,7] The bis(*N*-MeIm) complexes of Fe(III)BHP$^+$ and Fe(III)PFP$^+$ were obtained by dissolution of the chloride Fe(III) derivative in methylene chloride and addition of *N*-MeIm under vacuum. The ligand binding was checked by absorption and RR spectroscopies. For most of the investigated Fe(III)BHP$^+$ and Fe(III)PFP$^+$ complexes, the ligand concentrations were 0.1−1.0 mM. Preliminary titrations however showed that *N*-MeIm has low affinities for Fe(III)$[((C_4)_2\phi)_2]^+$, Fe(III) $[((C_3)_2\phi)(C_{12})]^+$, and Fe(III)$[((C_3)_2\phi)_2]^+$. A large ligand excess (1−8 M) was therefore necessary to form the bis(*N*-MeIm) complex of these Fe(III)BHP$^+$. The photoreduction of the Fe(III)-porphyrin complexes was checked by RR spectroscopy. *N*-MeIm (Sigma) and methylene chloride (Merck) were of spectroscopic grade.

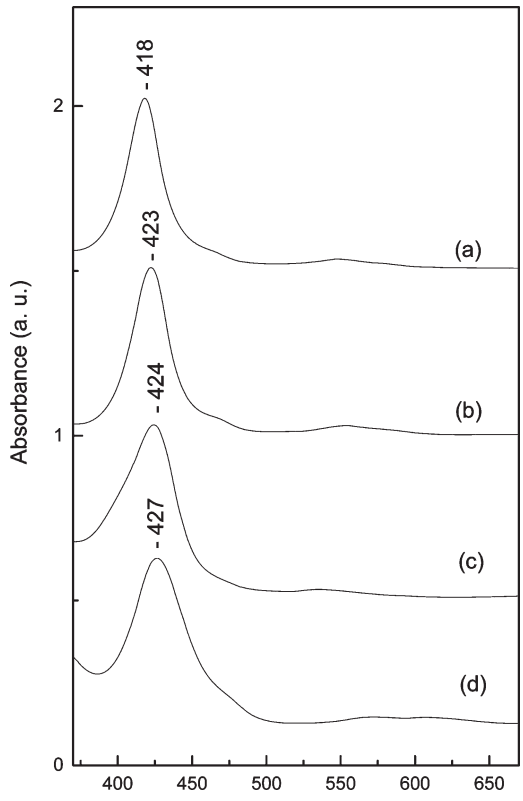

Figure 4. Visible absorption spectra (nm) of AC Fe(III)$[(C_4)_2\phi]_2$(*N*-MeIm)$_2^+$ (a), CT Fe(III)$[(C_4)_2\phi]_2$(*N*-MeIm)$_2^+$ (b), CT Fe(III)$[(C_3)_2\phi]$-$[C_{12}]$(*N*-MeIm)$_2^+$ (c), and CT Fe(III)$[(C_3)_2\phi]_2$(*N*-MeIm)$_2^+$ (d) in methylene chloride.

The electronic absorption spectra were measured by using a cary 5E (Varian) spectrometer. The EPR spectra were recorded at 15 K under nonsaturating microwave power with a Bruker ESP 300E X-band spectrometer equipped with an Oxford Instruments cryostats, a HP5350B microwave frequency counter, and a Bruker ER035 M NMR gaussmeter for the determination of the g values. The RR spectra were recorded at 20 ± 1 °C by using a Jobin-Yvon spectrometer (HG2S−UV) with the 441.6 nm excitation of a He−Cd laser (Liconix model 4050) and the 413.1 and 406.7 nm excitations of a Kr^+ ion laser (Coherent Innova). Using radiant powers of 10−50 mW, the RR spectra (10−15 scans) were independently collected and averaged. The spectral analysis was achieved by using a Grams 32 software (Galactic Industries). A mixture of benzene and methylene chloride (1/1 (v/v)) was used to calibrate the RR spectra. The frequencies of the RR bands of the Fe(III)BHP$^+$ and Fe(III)PFP$^+$ complexes were also internally calibrated against the ligand and solvent bands.

Results

Electronic Absorption Spectroscopy of the Bis(*N*-MeIm) Complexes of Fe(III)BHP$^+$ and Fe(III)PFP$^+$. Figure 4 shows the electronic absorption spectra of the bis(*N*-MeIm) complexes of AC Fe(III)$[(C_4)_2\phi]_2^+$, CT Fe(III)$[-((C_4)_2\phi)_2]^+$, CT Fe(III)$[((C_3)_2\phi)(C_{12})]^+$ and CT Fe(III)$[(-(C_3)_2\phi)_2]^+$. For these four complexes, the Soret band was gradually red-shifted from 418 nm for AC Fe(III)$[(C_4)_2\phi]_2$-(*N*-MeIm)$_2^+$ to 427 nm for CT Fe(III)$[((C_3)_2\phi)_2]$(*N*-MeIm)$_2^+$. The Soret band maximum of the bis(*N*-MeIm) complexes of Fe(III)TPP$^+$, CT Fe(III)$[(C_{11}\mathrm{Im})_2]_2^+$, AC Fe(III)$[((C_4)_2\phi)_2]^+$, and AC Fe(III)$[((C_3)_2\phi)_2]^+$ is observed

Table 2. Soret Band Maxima and EPR Parameters of Bis(*N*-Alkylimidazole) Complexes of Fe(III)TPP$^+$, CT, and AC Fe(III)BHP$^+$, and Fe(III)PFP$^+$

Fe(III) complexes	compound number	Soret maximum (nm)	EPR parameters				
			g_z	g_y	g_x	Δ/λ	ν/Δ
FeTPP(*N*-MeIm)$_2^+$	**1**	417	2.91	2.29	1.56	3.29	0.61
CT Fe[C_{11}Im]$_2^+$	**2**	417	2.89	2.30	1.48	2.85	0.67
CT Fe[$(C_4)_2\phi$]$_2$(*N*-MeIm)$_2^+$	**3**	423	3.18	2.17	1.37	3.50	0.41
CT Fe[$(C_3)_2\phi$][C_{12}](*N*-MeIm)$_2^+$	**4**	424	2.86	2.32	1.57	3.06	0.68
CT Fe[$(C_3)_2\phi$]$_2$(*N*-MeIm)$_2^+$	**5**	427	2.80	2.46	1.48	2.07	1.04
AC Fe[$(C_4)_2\phi$]$_2$(*N*-MeIm)$_2^+$	**6**	418	2.90	2.29	1.55	3.22	0.62
AC Fe[$(C_3)_2\phi$]$_2$(*N*-MeIm)$_2^+$	**7**	419	2.96	2.28	1.52	3.25	0.58
Fe[$\alpha\alpha\beta\beta$-T_{piv}PP](*N*-MeIm)$_2^+$	**8**	422	2.88	2.30	1.57	3.22	0.64
Fe[$\alpha\beta\alpha\beta$-T_{piv}PP](*N*-MeIm)$_2^+$	**9**	422	2.95	2.29	1.52	3.17	0.60

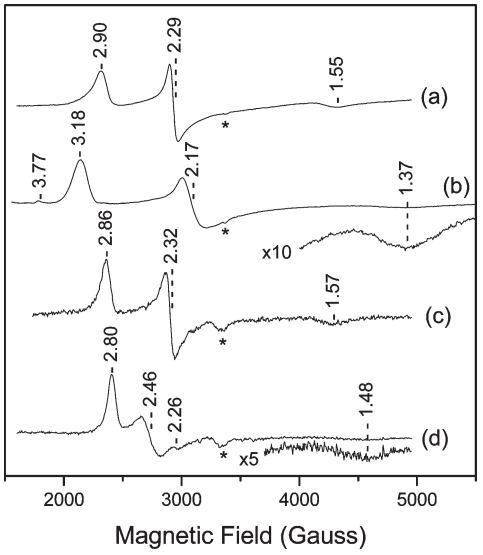

Figure 5. EPR spectra of AC Fe(III)[$(C_4)_2\phi$]$_2$(*N*-MeIm)$_2^+$ (a), CT Fe(III)[$(C_4)_2\phi$]$_2$(*N*-MeIm)$_2^+$ (b), CT Fe(III)[$(C_3)_2\phi$][C_{12}](*N*-MeIm)$_2^+$ (c), and CT Fe(III)[$(C_3)_2\phi$]$_2$(*N*-MeIm)$_2^+$ (d) in methylene chloride. The band marked with an asterisk is the result of a cavity signal.

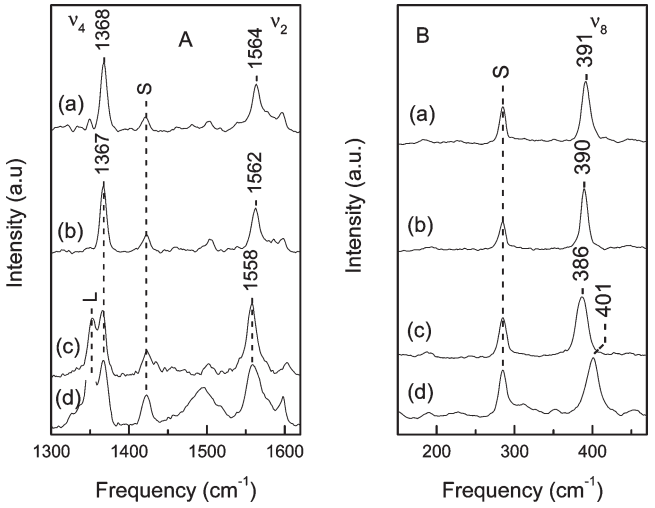

Figure 6. High- (1300−1620 cm^{-1}) (A) and low- (150−470 cm^{-1}) (B) frequency regions of RR spectra of AC Fe(III)[$(C_4)_2\phi$]$_2$(*N*-MeIm)$_2^+$ (a), CT Fe(III)[$(C_4)_2\phi$]$_2$(*N*-MeIm)$_2^+$ (b), CT Fe(III)[$(C_3)_2\phi$][C_{12}](*N*-MeIm)$_2^+$ (c), and CT Fe(III)[$(C_3)_2\phi$]$_2$(*N*-MeIm)$_2^+$ (d) in methylene chloride. Excitation: 413.1 nm; summations of 6−8 scans; S and L indicate solvent and ligand bands, respectively.

at 417−419 nm (spectra not shown; Table 1). That of the bis(*N*-MeIm) complexes of the Fe(III)PFP$^+$ is slightly red-shifted when compared to that of the Fe(III)TPP$^+$ complex, since it is observed at 422 nm for both the $\alpha\beta\alpha\beta$ and $\alpha\alpha\beta\beta$ atropisomers (Table 2).

Electron Paramagnetic Resonance Spectroscopy. The EPR spectra of CT Fe(III)[$(C_{11}Im)_2$](*N*-MeIm)$_2^+$ and AC Fe(III)[$((C_4)_2\phi)_2$](*N*-MeIm)$_2^+$ exhibit g_z, g_y, and g_x values at 2.89−2.90, 2.29−2.30, and 1.48−1.55, respectively. These values are comparable to those of the rhombic B-type hemichromes ($g_z \approx 2.9-3.0$, $g_y \approx 2.25-2.35$, and $g_x \approx 1.4-1.6$) (Figure 5, spectrum a; Table 2).[8] By contrast, the g values of the bis(*N*-MeIm) complex of CT Fe(III)[$((C_4)_2\phi)_2$]$^+$ ($g_z = 3.18$, $g_y = 2.17$, and $g_x = 1.37$) represent a highly anisotropic low-spin signature (Figure 5, spectrum b).[8b] For this complex, a minor species with a higher anisotropic character is even detected at $g = 3.77$ (Figure 5, spectrum b). As far as the bis(*N*-MeIm) complexes of CT Fe(III)[$(C_3)_2\phi$)(C_{12})]$^+$ and CT Fe(III)[$((C_3)_2\phi)_2$]$^+$ are concerned, a change in heme rhombicity is observed when the overall handle strain is increased (2.86 → 2.80 for g_{zz}, 2.32 → 2.46 for g_{yy}, and 1.57 → 1.48 for g_{xx}) (Figure 5, spectra c and d; Table 2). The bis(*N*-MeIm) complexes of Fe(III)TPP$^+$, AC Fe(III)[$((C_3)_2\phi)_2$]$^+$, Fe(III)[$\alpha\alpha\beta\beta$-T_{piv}PP]$^+$, and Fe(III)[$\alpha\beta\alpha\beta$-T_{piv}PP]$^+$ present typical B hemichrome spectra (Table 2).

Resonance Raman spectroscopy. The high- (1300−1620 cm^{-1}) and low- (150−450 cm^{-1}) frequency regions of the RR spectra of the bis(*N*-MeIm) complexes of AC Fe(III)-[$((C_4)_2\phi)_2$]$^+$, CT Fe(III)[$((C_4)_2\phi)_2$]$^+$, CT Fe(III)[$((C_3)_2\phi)$-(C_{12})]$^+$, and CT Fe(III)[$((C_3)_2\phi)_2$]$^+$ are displayed in Figure 6. While the oxidation state marker ν_4 mode was detected at a constant frequency (1367−1368 cm^{-1}), the ν_2 mode was downshifted from 1564 cm^{-1} for AC Fe(III) [$((C_4)_2\phi)_2$]$^+$, to 1562 cm^{-1} for CT Fe(III)[$((C_4)_2\phi)_2$]$^+$, 1559 cm^{-1} for CT Fe(III)[$((C_3)_2\phi)(C_{12})$]$^+$, and 1558 cm^{-1} for CT Fe(III)[$((C_3)_2\phi)_2$]$^+$ (Figure 6A). Similar gradual downshifts were observed for the ν_3 (1460 → 1459 → 1458 → 1457 cm^{-1}) and ν_{10} (1582 → 1580 → 1576 → 1576 cm^{-1}) modes when the strain on the handles is increased (Table 3). It is interesting to note that the ν_2, ν_3 and ν_{10} modes of the bis(*N*-MeIm) complex of Fe(III)TPP$^+$ were detected at 1563, 1460, and 1581 cm^{-1}, frequencies very close to those observed for CT Fe(III)[$(C_{11}Im)_2$]$^+$ (Table 3). Taking this set of frequencies as a reference, that of the bis(*N*-MeIm) complexes of AC Fe(III) [$((C_4)_2\phi)_2$]$^+$ and AC Fe(III)[$((C_3)_2\phi)_2$]$^+$ shows small positive

(8) (a) Peisach, J.; Blumberg, W. E.; Adler, A. *Ann. N.Y. Acad. Sci.* **1973**, *206*, 310. (b) Palmer, G. *Biochem. Soc. Trans.* **1985**, *13*, 548. (c) Walker, F. A.; Reis, D.; Balke, V. L. *J. Am. Chem. Soc.* **1984**, *106*, 6888. (d) Walker, F. A. *Coord. Chem. Rev.* **1999**, *185−186*, 471.

Table 3. RR Frequencies (cm^{-1}) of Bis(*N*-Alkylimidazole) Complexes of Fe(III)TPP$^+$, CT and AC Fe(III)BHP$^+$, and Fe(III)PFP$^+$

Fe(III) complexes	ν_4	ν_3	ν_{11}	ν_2	ν_{10}	ν_8
FeTPP(*N*-MeIm)$_2^+$	1367	1460	1501	1563	1581	391
CT Fe[C_{11}Im]$_2^+$	1368	1460	1501	1563	1582	390
CT Fe[$(C_4)_2\phi$]$_2$(*N*-MeIm)$_2^+$	1367	1459	1504	1562	1580	389
CT Fe[$(C_3)_2\phi$][C_{12}](*N*-MeIm)$_2^+$	1367	1458	1503	1559	1576	386
CT Fe[$(C_3)_2\phi$]$_2$(*N*-MeIm)$_2^+$	1367	1457	-	1558	1576	401
AC Fe[$(C_4)_2\phi$]$_2$(*N*-MeIm)$_2^+$	1368	1462	1505	1564	1577	391
AC Fe[$(C_3)_2\phi$]$_2$(*N*-MeIm)$_2^+$	1367	1463	1504	1563	1579	390
Fe[$\alpha\alpha\beta\beta$-T_{piv}PP](*N*-MeIm)$_2^+$	1367	1463	1505	1562	1579	386
Fe[$\alpha\beta\alpha\beta$-T_{piv}PP](*N*-MeIm)$_2^+$	1367	1461	1505	1562	1579	388

or negative deviations (1563−1564, 1462−1463 and 1577−1579 cm^{-1}, respectively) (Table 3).

In the low-frequency regions, the ν_8 mode of AC Fe(III)[$((C_4)_2\phi)_2$](*N*-MeIm)$_2^+$ was detected at 391 cm^{-1}, a frequency identical to that detected for the Fe(III)TPP(*N*-MeIm)$_2^+$ complex (Figure 6B, Table 3). A ν_8 frequency at 390 cm^{-1} was found for the bis(*N*-MeIm) complexes of CT Fe(III) [C_{11}Im]$_2^+$ and AC Fe(III) [$((C_3)_2\phi)_2$]$^+$ (Table 3). This frequency was gradually downshifted for the bis(*N*-MeIm) complexes of CT Fe(III)-[$((C_4)_2\phi)_2$]$^+$ (389 cm^{-1}), Fe(III)[$\alpha\beta\alpha\beta$-TpivPP]$^+$ (388 cm^{-1}), Fe(III)[$((C_3)_2\phi)(C_{12})$]$^+$ (386 cm^{-1}), and Fe(III)[$\alpha\alpha\beta\beta$-TpivPP]$^+$ (386 cm^{-1}) but was strongly upshifted at 401 cm^{-1} for the CT Fe(III)[$((C_3)_2\phi)_2$](*N*-MeIm)$_2^+$ complex (Figure 6B, Table 3).

Discussion

Absorption Spectroscopy. In general, the Soret band is red-shifted for the ferrous heme complexes compared to that of the ferric one. For the bis(*N*-MeIm) complexes of Fe(II)BHP, we showed that increased red-shifts of the Soret band were the result of increased ruffling themselves because of a decreased length of the porphyrin handles.[5a] We recall that the porphyrin core of the reference unconstrained model, that is, Fe(II)TPP(*N*-MeIm)$_2$, is planar.[3d] Considering the bis(*N*-MeIm) complexes of the ferric forms, the situation differs from that met for the ferrous compounds since the core conformation of FeTPP(*N*-MeIm)$_2$ is sensitive to the oxidation state of the iron atom. In the absence of steric effect resulting from either the axial ligands or the porphyrin substituents, bis-imidazole complexes of Fe(III)-porphyrins exhibit an average Fe−N(pyrrole) distance (1.979 Å) that is only shorter by 0.023 Å than the average distance of the Fe(II) analogs.[2,3] The ferrous complexes adopt a planar porphyrin conformation. The equatorial bond shortening of ca. 0.02 Å results in a core ruffling of the Fe(III) species. In particular, the porphyrin core of the bis(*N*-MeIm) complexes of ferriprotoporphyrin IX and Fe(III)TPP$^+$ is ruffled.[2b,e] Therefore, the porphyrin core of our reference model, that is, Fe(III)TPP((*N*-MeIm)$_2^+$, is distorted. Taking into account the fact that the investigated Fe(III)TPP$^+$, Fe(III)BHP$^+$, and Fe(III)PFP$^+$ complexes have all two *N*-alkylimidazole ligands and are dissolved in the same solvent, red-shifts of the Soret band are thus indicative of an increased distortion of the porphyrin macrocycle (Table 2). However, these changes in Soret position do not discriminate the deformation type. Since we observe no blue-shift of the Soret band, none of the ferric complexes presented in Table 2 could adopt a planar heme structure.

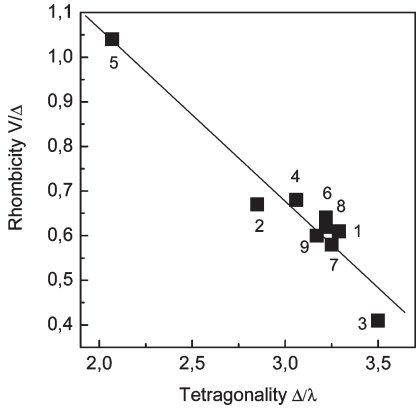

Figure 7. Rhombicity (V/Δ) versus tetragonality (Δ/λ) for the bis(*N*-alkylimidazole) complexes of Fe(III)TPP$^+$, CT and AC Fe(III)BHP$^+$, and FePFP$^+$ complexes. The compound numbering is indicated in Table 2.

Electron Paramagnetic Resonance Spectroscopy. The *g* values observed for the Fe(III)BHP$^+$ and Fe(III)PFP$^+$ complexes in frozen solution provides a measure of the symmetry of the Fe(III) coordination. Table 2 lists the rhombicity (V/Δ) and the tetragonality (Δ/λ) of the complexes deduced from the *g* values. The V/Δ versus Δ/λ plot of the investigated complexes shows a linear correlation (Figure 7). Most of the complexes have rhombic typical B hemichrome signature with the rhombicity $V/\Delta = 0.58-0.68$ and the tetragonality $\Delta/\lambda = 3.0-3.3$.[8] The points corresponding to the bis(*N*-MeIm) complexes of CT Fe(III)[$((C_4)_2\phi)_2$]$^+$ ($V/\Delta = 0.41$, $\Delta/\lambda = 3.50$) and CT Fe(III)[$((C_3)_2\phi)_2$]$^+$ ($V/\Delta = 1.04$, $\Delta/\lambda = 2.07$) are outside the B domain defined by Blumberg and Peisach[8a] and constitutes two notable exceptions. Indeed, the major species of CT Fe(III)[$((C_4)_2\phi)_2$](*N*-MeIm)$_2^+$ exhibits a g_{max} value at 3.18 indicative of a "highly anisotropic low-spin " or "large g_{max}" type I EPR signals. A rough linear relationship between g_z or g_{max} and the dihedral angle between the axial ligand planes ($\Delta\varphi$) has been recently established.[9] From this correlation, a $\Delta\varphi$ value of ∼50° is deduced. The g_{max} value of the minor species of CT Fe(III)[$((C_4)_2\phi)_2$](*N*-MeIm)$_2^+$ (3.77) is close to the highest possible value for low-spin Fe(III) complexes (∼3.8)[10] and represents a $\Delta\varphi$ dihedral angle close to 90°. The lowest *g* value of the CT Fe(III)[$((C_3)_2\phi)_2$]](*N*-MeIm)$_2^+$ complex ($g_z = 2.80$) is assignable to a rhombic type II signal.[8] According to the relationship g_z versus $\Delta\varphi$, it can be associated with nearly parallel axial rings, that is, a $\Delta\varphi$ angle between 0° and 10°.[9] With a g_z value at 2.86, the EPR signal of bis(*N*-MeIm) complex of CT Fe(III)[$((C_3)_2\phi)(C_{12})$]$^+$ is also rhombic with nearly parallel ligand rings ($\Delta\varphi$ of ∼10°).

From the EPR data shown above, it appears that the shortening of at least one handle from [$((C_4)_2\phi)_2$] to [$((C_3)_2\phi)_2)(C_{12})$] or [$((C_3)_2\phi)_2$] in the CT Fe(III)BHP$^+$ complexes produce an important shutting of the dihedral angle formed by the axial rings. The bis(*N*-MeIm) complexes of CT Fe(III)[C_{11}Im]$_2^+$, AC Fe(III)[$((C_4)_2\phi)_2$]$^+$,

(9) (a) Teschner, T.; Yatsunyk, L.; Schünemann, V.; Paulsen, H.; Winkler, H.; Hu, C.; Scheidt, W. R.; Walker, F. A.; Trautwein, A. X. *J. Am. Chem. Soc.* **2006**, *128*, 1379. (b) Yatsunyk, L. A.; Dawson, A.; Carducci, M. D.; Nichol, G. S.; Walker, F. A. *Inorg. Chem.* **2006**, *45*, 5417.

(10) Lindsey, J. S.; Wagner, R. W. *J. Org. Chem.* **1989**, *54*, 828.

Fe(III)[$\alpha\alpha\beta\beta$-T_{piv}PP]$^+$, and Fe(III)TPP$^+$ have g_z values of 2.88−2.91 and are attributed to $\Delta\varphi$ angles of 10°-20°, in agreement with the crystallographic data obtained for the Fe(III)-protoporphyrin(*N*-MeIm)$_2^+$ and Fe(III)TPP-(*N*-MeIm)$_2^+$ complexes ($\Delta\varphi = 11-13°$). This angle opening is most likely increased in the 20−30° range for the AC Fe(III)[$((C_3)_2\phi)_2$]$^+$ and Fe(III)[$\alpha\beta\alpha\beta$-T_{piv}PP]$^+$ complexes ($g_z = 2.95-2.96$).

Resonance Raman Spectroscopy. The ν_4 RR mode which was assigned to a half-ring pyrrole breathing mode is an indicator of the oxidation and coordination state of the iron atom.[11,12] With a frequency observed at 1367−1368 cm^{-1} (Table 3), it confirms that all the bis-(*N*-MeIm) complexes of FeBHP, FePFP and FeTPP which were investigated here are ferric, six-coordinated and low-spin. In our previous study on the bis(*N*-MeIm) complexes of the homologous ferrous complexes,[5] we showed that the ν_2 and ν_8 modes are good markers of the porphyrin conformation. The ν_2 mode was calculated to be a mixing of C_bC_b and C_aC_m stretching.[11] However, its high sensitivity to porphyrin ruffling suggests a predominant C_aC_m stretching in its potential energy distribution.[13] The ν_8 RR mode involves primarily Fe−N(pyrrole) and C_aC_m stretching motion and methine bridge bending ($\delta(C_aC_mC_a)$).[11] Its frequency is thus sensitive to changes in porphyrin conformation because of changes in Fe−N(pyrrole) bond distance and angular deformations of the methine bridges. This mode is likely more affected to all types of porphyrin deformation than ν_2. Therefore, the high-frequency ν_2 mode and the low-frequency ν_8 mode are expected to measure different aspects of the changes in porphyrin conformation induced by changes in steric and electronic interactions of the Fe-porphyrin system with its superstructure and its ligands.

Heme Structure in the Fe(III)BHP$^+$ Complexes. The type and extent of porphyrin distortions depend on an energetic compromise between the size of the metal ion and the constrains exerted by the ligand rings and the porphyrin superstructures on the tetrapyrrole.[5a] Considering the decreased ionic radii of the iron atom upon its oxidation,[14] the mutual interactions between ligands, superstructure, and Fe-heme are most likely different in the Fe(II) and Fe(III) series. The observation of very low ligand affinities for the most strained CT Fe(III)BHP$^+$ complexes supports this hypothesis. Saddling and ruffling are the most plausible heme conformations for Fe-porphyrin(*N*-MeIm)$_2$ complexes (Figure 1, panels A and B). However, the strength of the peripheral strains and the asymmetry of these strains can promote other out-of-plane (oop) types of nonplanar distortions, such as waving and doming (Figure 1, panels C and D).

Both the Fe−N(pyrrole) bonds and the methine bridges are strongly affected by porphyrin distortion. Ruffling causes strong $NC_aC_mC_a$ torsions allowing a shortening of the Fe−N(pyrrole) bonds. Saddling does not cause twisting about the C_aC_m bonds, the four C_m atoms remaining coplanar with the metal ion. Ruffling and saddling shorten the Fe−N(pyrrole) bonds but ruffling tends to contract the porphyrin core more than saddling.[15] Doming causes lengthening of the Fe−N-(pyrrole) bonds but does not twist the C_aC_m bonds. Waving is a chairlike conformation. Two opposite pyrrole rings are tilted up and down with respect to the mean porphyrin plane. The other pyrrole rings are rotated in the same direction around their median lines (Figure 1C). This deformation type allows the stabilization of short Fe−N(pyrrole) bonds and affects the $C_aC_mC_a$ angles by pair. Two adjacent C_m atoms are above the porphyrin plane while the two others are under this plane.

The phenyl−porphyrin interactions are also differently affected by the oop deformations of the tetraarylporphyrins.[16] The phenyl groups of a ruffled tetraphenylporphyrin are perpendicular to the $C_aC_mC_a$ plane. Since the C_m atoms are alternatively above and below the mean porphyrin plane, they point alternatively up and down of the porphyrin plane. The phenyl rings associated to a saddled macrocycle are alternately tilted left and right with respect to the $C_aC_mC_a$ planes. In a waved structure, two adjacent phenyl rings are tilt in one direction and the other two in opposite direction so that opposite phenyl rings eclipse. The phenyl rings of a domed Fe-porphyrin are perpendicular to the $C_aC_mC_a$ plane and thus the mean porphyrin plane. A short CT connection in the CT FeBHP complexes allows the displacement of opposite phenyl rings up or down the mean porphyrin plane, severely limiting the ring tilting and thus stabilizing a ruffled structure. When the length of the CT links is increased, small phenyl tiltings are allowed and a mixing of ruffled and saddled conformations can occur. The adjacent-cis links in AC FeBHP complexes can limit or hinder the rotation and the tilting in opposite direction of two adjacent phenyl rings and thus can favor a waved conformation. Phenyl tilting is mostly allowed in the FePFP complexes and thus can stabilize saddled and waved conformations.

When compared to the Soret maximum of Fe(III)TPP-(*N*-MeIm)$_2^+$ (417 nm), the CT Fe(III)[$(C_4)_2\phi$]$_2$(*N*-MeIm)$_2^+$ complex shows a marked change at 423 nm. This red-shift is associated with an increased heme deformation.[5,17] The small downshift of the ν_8 frequency (389 cm^{-1} versus 391 cm^{-1} for the Fe(III)TPP(*N*-MeIm)$_2^+$ complex) indicates that this change in heme conformation is not a ruffling for which an increased in ν_8

(11) (a) Li, X.-Y.; Czernuszewicz, R. S.; Kincaid, J. R.; Su, Y. O.; Spiro, T. G. *J. Phys. Chem.* **1990**, *94*, 31. (b) Li, X.-Y.; Czernuszewicz, R. S.; Kincaid, J. R.; Stein, P.; Spiro, T. G. *J. Phys. Chem.* **1990**, *94*, 47.

(12) (a) Burke, J. M.; Kincaid, J. R.; Peters, S.; Gagne, R. R.; Collman, J. P.; Spiro, T. G. *J. Am. Chem. Soc.* **1978**, *100*, 6083. (b) Parthasarathi, N.; Hansen, C.; Yamaguchi, S.; Spiro, T. G. *J. Am. Chem. Soc.* **1987**, *109*, 3865.

(13) (a) Jentzen, W.; Simpson, M. C.; Hobbs, J. D.; Song, X.; Ema, T.; Nelson, N. Y.; Medforth, C. J.; Smith, k. M.; Veyrat, M.; Mazzanti, M.; Ramasseul, R.; Marchon, j. C.; Takeuchi, T.; Goddard, W. A., III; Shelnutt, J. A. *J. Am. Chem. Soc.* **1995**, *117*, 11085. (b) Franco, R.; Ma, J.-G.; Lu, Y.; Ferreira, G. C.; Shelnutt, J. A. *Biochemistry* **2000**, *39*, 2517.

(14) Shannon, R. D. *Acta Crystallogr.* **1976**, *A32*, 751.

(15) Song, X.-Z.; Jaquinod, L.; Jentzen, W.; Nurco, D. J.; Jia, S.-L.; Khoury, R. G.; Ma, J.-G.; Medforth, C. J.; Smith, K. M.; Shelnutt, J. A. *Inorg. Chem.* **1998**, *37*, 2009.

(16) (a) Scheidt, W. R.; Lee, Y. J. *Struct. Bonding* (*Berlin*) **1987**, *64*, 1. (b) Jentzen, W.; Unger, E.; Song, X.-Z.; Jia, S.-L.; Turowska-Tyrk, I.; Schweitzer-Stenner, R.; Dreybrodt, W.; Scheidt, W. R. *J. Phys. Chem. A* **1997**, *101*, 5789. (c) Nurco, D. J.; Medforth, C. J.; Forsyth, T.; Olmstead, M. M.; Smith, K. M. *J. Am. Chem. Soc.* **1996**, *118*, 10918.

(17) (a) Barkigia, K. M.; Chantranupong, L.; Smith, k. M.; Fajer, J. *J. Am. Chem. Soc.* **1988**, *110*, 7566. (b) Haddad, R. E.; Gazeau, S.; Pécaut, J.; Marchon, J. C.; Medforth, C. J.; Shelnutt, J. A. *J. Am. Chem. Soc.* **2003**, *125*, 1253.

frequency is expected.[5a] The flexible and long $(C_4)_2\phi$ chains allow small rotations of the meso phenyl groups in opposite direction and thus can stabilize a saddling contribution. As a consequence, the tilting of opposite pyrrole rings permits an arrangement of the axial imidazole rings with an angle of ca. 50°. A mixing of ruffled and saddled structures in CT Fe(III)$[(C_4)_2\phi]_2(N\text{-MeIm})_2^+$ is plausible considering the small sensitivity of the ν_2 mode for saddling.[13]

The CT Fe(III)$[(C_3)_2\phi]_2$ $(N\text{-MeIm})_2^+$ complex exhibits the most important spectral changes when compared to Fe(III)TPP$(N\text{-MeIm})_2^+$. The Soret maximum is shifted by 10 nm and the ν_2 and ν_8 modes by -5 and $+10$ cm^{-1}, respectively (Tables 2 and 3). A strong red-shift of the Soret transition coupled to a strong downshift of ν_2 and a stronger upshift of ν_8 are spectral criteria of a strong increase in porphyrin ruffling.[5] The short CT $(C_3)_2\phi$ chains generate oop positions of opposite C_m atoms, blocking phenyl rotations and thus favoring a strong porphyrin ruffling. From the EPR measurements, we deduced that the axial imidazole rings are nearly parallel. No Fe-porphyrin complex combining such an axial arrangement with a strongly ruffled macrocycle has been described. Up to now, crystal structures of bis(5-methylimidazole) complexes of Fe(III)-tetramesitylporphyrin have revealed the combination of a moderate heme ruffling with parallel ligand rings.[18]

The Soret band position of the CT Fe(III)$[(C_3)_2\phi][C_{12}]$-$(N\text{-MeIm})_2^+$ complex is shifted by 7 nm in comparison to that of Fe(III)TPP$(N\text{-MeIm})_2^+$ (424 versus 417 nm). This red-shift again indicates an important difference in porphyrin conformation. As far as the RR modes are concerned, ν_2 and ν_8 are downshifted by 4 and 5 cm^{-1}, respectively. The behavior of the ν_8 mode allows us to discard any increase in porphyrin ruffling. A negative shift of ν_8 is associated with a lengthening of the Fe−N(pyrrole) bonds produced by a domed contribution. The superstructure of CT Fe$[(C_3)_2\phi][C_{12}](N\text{-MeIm})_2^+$ complex is asymmetric since it contains a short and relatively rigid $(C_3)_2\phi$ handle and a long and loose C_{12} handle. As a consequence of this handle asymmetry, a gabbled structure,[19] that is, a mixing of porphyrin ruffling with a small doming toward the longest C_{12} chain, can alleviate the steric interactions between the shortest $(C_3)_2\phi$ handle and the axial imidazole ring.

The CT Fe(III)$[C_{11}Im]_2^+$, AC Fe(III)$[(C_4)_2\phi]_2(N\text{-MeIm})_2^+$, and AC Fe(III)$[(C_3)_2\phi]_2(N\text{-MeIm})_2^+$ complexes present spectral parameters very close to those of Fe(III)TPP$(N\text{-MeIm})_2^+$ (Soret bands at 417−419 nm; ν_2 at 1563−1564 cm^{-1}; ν_8 at 390−391 cm^{-1}). The CT Fe(III)$[C_{11}Im]_2^+$ molecule likely adopts a small porphyrin ruffling similar to that of Fe(III)TPP$(N\text{-MeIm})_2^+$, long CT links having no determinant role in the stabilization of one of the other possible porphyrin conformers. As far as the AC Fe(III)$[(C_4)_2\phi]_2^+$ and AC Fe$[(C_3)_2\phi]_2^+$ complexes are concerned, the AC handles restrain or even prevent: (i) the rotation in opposite direction of the linked phenyl rings, thus destabilizing heme saddling and (ii) the displacement of opposite phenyl rings up (or down) the mean porphyrin plane, thus disfavoring heme ruffling. Thus, a moderate heme waving most likely occurs for the AC Fe(III)$[(C_4)_2\phi]_2^+$ and AC Fe(III)$[(C_3)_2\phi]_2^+$ complexes.

Heme Structure in the Fe(III)PFP$^+$ Derivatives. The Soret band positions and the ν_8 frequencies of the bis(*N*-MeIm) complexes of Fe(III)$T_{piv}PP^+$ and Fe(III)TPP^+ are clearly distinct (Soret at 422 nm versus 417 nm and ν_8 at 386−388 cm^{-1} versus 391 cm^{-1}). They indicate different conformations for the ferriheme of the Fe(III)$T_{piv}PP^+$ and Fe(III)TPP^+ complexes. We cannot conclude for a smaller ruffling for the Fe(III)$T_{piv}PP^+$ complexes when compared to that of the Fe(III)TPP^+ complex if one consider together the Soret (+5 nm), ν_2 (-1 cm^{-1}), and ν_8 ($-3-5$ cm^{-1}) shifts. A decreased ruffling would blue-shift the Soret band and increase the ν_2 frequency. This is not the case. Considering that the ν_2 frequency is much more sensitive to ruffling than other oop deformations,[13] a porphyrin saddling and/or waving in the Fe(III)$T_{piv}PP^+$ complexes could account for the observed spectral properties. We previously observed a trend for heme saddling upon ligand strains in Fe(II) [$\alpha\beta\alpha\beta$-$T_{piv}PP$] complexes.[5b]

Redox Conformational Changes of the Heme in the Bis(*N*-MeIm) Complexes of FeBHP and FePFP. Structural results on hemoproteins, in which heme is coordinated by two histidine residues show that the polypeptide chain exerts a major effect on the axial imidazole rings.[20] In fact, a large variety of relative orientation was observed ($\Delta\varphi = 0-90°$). Except the globin fold, there is no systematic relationship between the relative orientation of the axial histidine and the protein structure.[20b] The histidine ligation itself affects the heme conformation since it induces larger distortion from planarity than other natural ligands. The influence of the oxidation state of the iron atom on these heme deformations is unfortunately not determined.[20b] This limitation in structural data justifies a spectroscopic approach.

As described above, the iron oxidation in bis(imidazole) and bis(*N*-MeIm) complexes of Fe-porphyrins produces a shortening of the axial and equatorial Fe−N bonds.[2,3,21] This effect reflects the similar antibonding orbital populations for the two oxidation states.[22] In addition to the smaller radius for the Fe(III) ion, the shorter mean Fe−N(pyrrole) distances for the ferric complexes reflect the fact that most of the Fe-porphyrinate complexes have a planar heme in the ferrous state and a ruffled heme in the oxidized state. An exception concerns bis(2-methylimidazole) and bis(1,2-dimethylimidazole) complexes that are ruffled in both oxidation states.[21,23] This heme deformation originates from strong steric interactions between the ligand 2-methyl group and the porphyrin. Because of the limited

(18) Munro, O. Q.; Serth-Guzzo, J. A.; Turowska-Tyrk, I.; Mohanrao, K.; Shokhireva, T. K.; Walker, F. A.; Debrunner, P. G.; Scheidt, W. R. *J. Am. Chem. Soc.* **1999**, *121*, 11144.

(19) Song, X.-Z.; Jentzen, W.; Jia, S.-L.; Jaquinod, L.; Nurco, D. J.; Medforth, C. J.; Smith, K. M.; Shelnutt, J. A. *J. Am. Chem. Soc.* **1996**, *118*, 12975.

(20) (a) Zarić, S. D.; Popović, D. M.; Knapp, E.-W. *Biochemistry* **2001**, *40*, 7914. (b) Merlino, A.; Vergara, A.; Sica, F.; Mazzarella, L. *Mar. Genomics* **2009**, *2*, 51.

(21) Hu, C.; Noll, B. C.; Schulz, C. E.; Scheidt, W. R. *Inorg. Chem.* **2005**, *44*, 4346.

(22) Scheidt, W. R.; Reed, C. A. *Chem. Rev.* **1981**, *81*, 543.

(23) (a) Scheidt, W. R.; Kirner, J. F.; Hoard, J. L.; Reed, C. A. *J. Am. Chem. Soc.* **1987**, *109*, 1963–1968. (b) Munro, O. Q.; Marques, H. M.; Debrunner, P. G.; Mohanrao, K.; Scheidt, W. R. *J. Am. Chem. Soc.* **1995**, *117*, 935.

Table 4. Redox Sensitivities of the Soret Band and the ν_2 and ν_8 RR Modes of the Bis(*N*-Alkylimidazole) Complexes of FeTPP, CT and AC FeBHP, and FePFP

	Soret maximum (nm)			ν_2 (cm^{-1})			ν_8 (cm^{-1})		
Fe-porphyrin complexes	Fe(II)	Fe(III)	ΔSoret	Fe(II)	Fe(III)	$\Delta\nu_2$	Fe(II)	Fe(III)	$\Delta\nu_8$
FeTPP(*N*-MeIm)$_2$	427	417	−10	1558	1563	+5	383	391	+8
CT Fe[C_{11}Im]$_2$	428	417	−11	1560	1563	+3	381	390	+9
CT Fe[$(C_4)_2\phi$]$_2$ (*N*-MeIm)$_2$	432	423	−9	1558	1562	+4	383	389	+6
CT Fe[$(C_3)_2\phi$][C_{12}] (*N*-MeIm)$_2$	434	424	−10	1556	1559	+3	384	386	+2
CT Fe[$(C_3)_2\phi$]$_2$ (*N*-MeIm)$_2$	440	427	−13	1553	1558	+5	389	401	+12
AC Fe[$(C_4)_2\phi$]$_2$ (*N*-MeIm)$_2$	428	418	−10	1559	1564	+5	384	391	+7
AC Fe[$(C_3)_2\phi$]$_2$ (*N*-MeIm)$_2$	428	419	−9	1559	1563	−4	383	390	+7
Fe[$\alpha\alpha\beta\beta$-T_{piv}PP] (*N*-MeIm)$_2$	428	422	−6	1558	1562	+4	381	386	+5
Fe[$\alpha\beta\alpha\beta$-T_{piv}PP] (*N*-MeIm)$_2$	428	422	-6	1558	1562	+4	383	388	+5

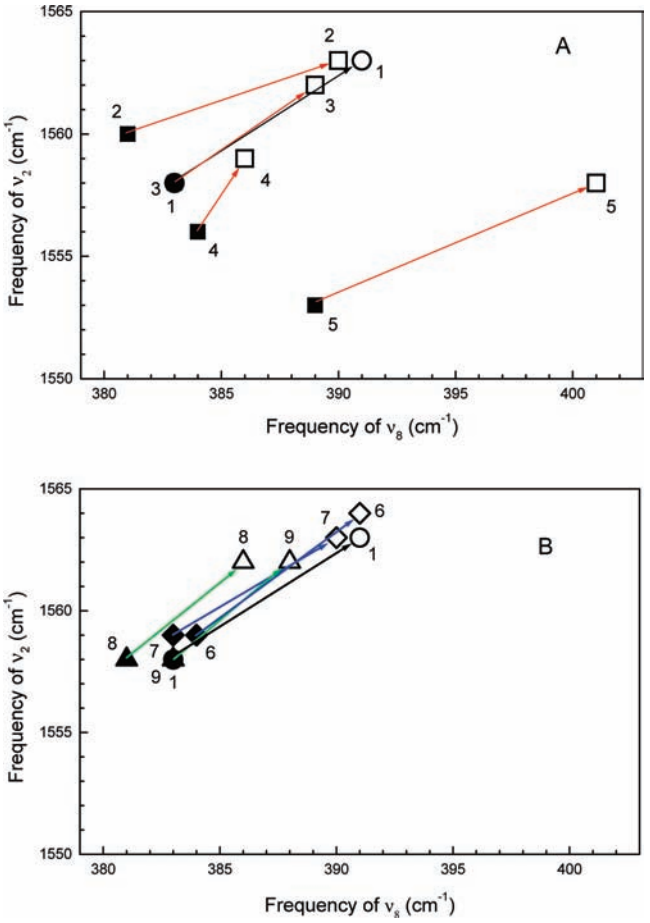

Figure 8. ν_2/ν_8 correlations for the bis(*N*-alkylimidazole) complexes of reduced and oxidized FeTPP, CT and AC FeBHP, and FePFP. Panel A: FeTPP and CT FeBHP complexes. Panel B: FeTPP, AC FeBHP, and FePFP complexes. The compound numbering is indicated in Table 2. The filled and open symbols correspond to the reduced and oxidized states, respectively.

number of investigated model complexes, the changes in heme ruffling and in Fe−N(pyrrole) bond length upon iron oxidation are however not clear.[24] Bis(pyridine) complexes of strained Fe(II)-porphyrins exhibit a saddled or a ruffled heme, but no structural information is available for the ferric state.[25] Therefore, the structural changes induced by iron oxidation of a heme already distorted in the ferrous state are not clearly determined. More generally, few crystal determinations of the ferrous and ferric forms of the same complex have been carried out.

Table 5. Slope (*S*) and Length (*L*) of the Fe(II) → Fe(III) Redox Transitions of the Bis(*N*-Alkylimidazole) Complexes of FeTPP, CT and AC FeBHP, and FePFP (see Figure 8A and B)

Fe(II) → Fe(III) complex	*S*	*L* (cm^{-1})
FeTPP(*N*-MeIm)$_2$	0.62	9.4
CT Fe[C_{11}Im]$_2$	0.33	9.5
CT Fe[$(C_4)_2\phi$]$_2$(*N*-MeIm)$_2$	0.66	7.2
CT Fe[$(C_3)_2\phi$][C_{12}](*N*-MeIm)$_2$	1.50	3.6
CT Fe[$(C_3)_2\phi$]$_2$(*N*-MeIm)$_2$	0.42	13
AC Fe[$(C_4)_2\phi$]$_2$(*N*-MeIm)$_2$	0.71	8.6
AC Fe[$(C_3)_2\phi$]$_2$(*N*-MeIm)$_2$	0.57	8.1
Fe[$\alpha\alpha\beta\beta$-TpivPP](*N*-MeIm)$_2$	0.80	6.4
Fe[$\alpha\beta\alpha\beta$-TpivPP](*N*-MeIm)$_2$	0.80	6.4

From the present spectroscopic results and those previously published,[5] it is interesting to investigate the redox behavior of the superstructured FeBHP and FePFP complexes. For this purpose, we propose to evaluate the extent and nature of the structural changes of heme upon iron oxidation by using the shifts of the Soret absorption bands and the ν_2 and ν_8 RR bands (Table 4). Moreover, the frequencies of the structure-sensitive ν_2 and ν_8 lines allow us to estimate the extent of porphyrin structural changes when the iron atom is oxidized. In Figure 8, the ν_2 and ν_8 frequencies of the Fe(II)- and Fe(III)-porphyrin complexes were plotted. For each redox couple, the length (*L*), as well as the slope (*S*), of the vector joining the point corresponding to the reduced state to that corresponding to the oxidized state were measured to describe the structural redox transition (Figure 8A,B; Table 5). Taking the spectral shifts observed for the Fe(II)TPP(*N*-MeIm)$_2$ → Fe(III)TPP(*N*-MeIm)$_2^+$ redox transition as a reference (Δ*S*oret = −10 nm, $\Delta\nu_2$ = +5 cm^{-1}, and $\Delta\nu_8$ = +8 cm^{-1}), Table 4 shows different types of behaviors for the FeBHP and FePFP complexes.

The CT Fe[C_{11}Im]$_2$ system exhibits spectral changes very similar to those of the FeTPP complexes (ΔSoret = −10−11 nm, $\Delta\nu_2$ = 3−5 cm^{-1}, and $\Delta\nu_8$ = 8−9 cm^{-1}) that could indicate very similar changes in heme structure for the two Fe-porphyrins. The ν_2/ν_8 relationship however shows that the redox transitions differ in terms of *S* values (0.33 versus 0.62), the *L* values being practically constant (9.4−9.5 cm^{-1}) (Table 5). This effect is related to the fact

(24) The displacement of the meso carbons (ΔC_m) from the mean porphyrin plane measures the porphyrin ruffling. ΔC_m is 0.50−0.51 Å for Fe(II)TMP(2MeHIm)$_2$, 0.40 Å for Fe(III)TPP(2MeHIm)$_2$, and 0.70 Å for Fe(III)TMP(1,2Me$_2$Im)$_2$.[21,23]

(25) (a) Grinstaff, M. W.; Hill, M. G.; Birnbaum, E. R.; Schaefer, W. P.; Labinger, J. A.; Gray, H. B. *Inorg. Chem.* **1995**, *34*, 4896. (b) Moore, K. T.; Fletcher, J. T.; Therien, M. *J. Am. Chem. Soc.* **1999**, *121*, 5196.

that the most important structural difference between the FeTPP(*N*-MeIm)$_2$ and CT Fe[C_{11}Im]$_2$ redox couples concerns the ferrous states, the heme of the Fe(II)[C_{11}Im]$_2$ system appearing more planar than that of the Fe(II)TPP(*N*-MeIm)$_2$ complex.[5a]

The CT Fe[((C_4)$_2\phi$)$_2$] complexes exhibit similar spectral shifts when compared to those of the FeTPP complexes (ΔSoret = -9 vs -10 nm, $\Delta\nu_2 = 4$ vs 5 cm^{-1}, and $\Delta\nu_8 = 6$ vs 8 cm^{-1}). The ν_2/ν_8 relationship show slopes nearly identical for the two complexes ($S = 0.62-0.66$) but a shorter run for CT Fe[((C_4)$_2\phi$)$_2$] ($L = 7.2$ vs 9.4 cm^{-1}). The main structural changes upon redox change concern the ferric states for which a mixture of ruffling and saddling is proposed.

The CT Fe[(C_3)$_2\phi$] [C_{12}] complexes display a normal Soret shift (ΔSoret = -10 nm) but small Raman shifts ($\Delta\nu_2$ and $\Delta\nu_8$ = 2 cm^{-1}). Among the investigated complexes, the redox change in the CT Fe[(C_3)$_2\phi$][C_{12}] complexes produces the smallest length ($L = 3.6$ cm^{-1}) and the highest slope (S = 1.50) (Table 5). Recalling that ν_2 is primarily associated with $\nu(C_aC_m)$ and ν_8 with ν(Fe$-$N(pyrrole), these values correspond to a decreased core size that is impeded by an increase in Fe$-$N(pyrrole) bond length. These effects are assigned to a structural transition from ruffled for the ferrous state to gabbled for the ferric state.

The CT Fe[(C_3)$_2\phi$)$_2$](*N*-MeIm)$_2$ complexes present strong shifts for the Soret transition (ΔSoret = -13 nm) as well as for the RR modes, in particular ν_8 ($\Delta\nu_2 = 5$ cm^{-1}; $\Delta\nu_8 = 12$ cm^{-1})(Table 4). The redox transition in the CT Fe[((C_3)$_2\phi$)$_2$](*N*-MeIm)$_2$ system induces the longest shift (L = 13 cm^{-1}) with a small slope ($S = 0.42$) (Table 5). The Soret, ν_2, and ν_8 variations are all in agreement with a strong increase in heme ruffling upon iron oxidation.[5a]

The AC Fe[((C_4)$_2\phi$)$_2$] and AC Fe[((C_3)$_2\phi$)$_2$] complexes exhibit spectral shifts very similar to those of the FeTPP complexes (ΔSoret = $-9-10$ nm, $\Delta\nu_2 = 4-5$ cm^{-1}, and $\Delta\nu_8 = 7-8$ cm^{-1}) indicating structural changes in terms of energy similar for these complexes and for FeTPP. The macrocycle of AC Fe(II)[((C_4)$_2\phi$)$_2$](*N*-MeIm)$_2$ and AC Fe(II)[((C_3)$_2\phi$)$_2$](*N*-MeIm)$_2$ complexes was proposed to be planar like that of Fe(II)TPP(*N*-MeIm)$_2$.[5a] The core of AC Fe(III)[((C_4)$_2\phi$)$_2$](*N*-MeIm)$_2^+$ and AC Fe(III)-[((C_3)$_2\phi$)$_2$](*N*-MeIm)$_2^+$ complexes could be ruffled like that of Fe(III)TPP(*N*-MeIm)$_2^+$.[2] However, these complexes are most likely slightly waved if we consider that the AC links do not stabilize the ruffled conformation.

The Fe[$\alpha\alpha\beta\beta$-T_{piv}PP](*N*-MeIm)$_2$ and Fe[$\alpha\beta\alpha\beta$-T_{piv}PP](*N*-MeIm)$_2$ complexes exhibit small shifts for the Soret band (-6 nm) and the ν_8 mode ($+5$ cm^{-1})(Table 4). For these complexes, the S and L values (0.80 and 6.4 cm^{-1}, respectively) differ from those of the FeTPP-(*N*-MeIm)$_2$ redox couple (0.62 and 9.4 cm^{-1}). This profile shows that the heme conformational change upon iron oxidation of the FeT_{piv}PP(*N*-MeIm)$_2$ derivatives is smaller than that of the FeTPP(*N*-MeIm)$_2$ complexes. The high S value and the low L value of the FePFP derivatives are indicative of a decreased core size that is not totally the result of a decrease in Fe$-$N(pyrrole) bond length. Considering the absolute positions of the Soret band and the ν_8 mode of the FeT_{piv}PP and FeTPP complexes, differences in heme structure mainly concern the ferric form since the spectral parameters of the ferrous forms correspond to a planar structure for the Fe(II)T_{piv}PP complexes.[5b] Thus, a change from planar for the Fe(II)PFP complexes to saddled or waved for the Fe(III)PFP$^+$ complexes can account for the S and L values.

In conclusion, Figure 8 illustrates the complexity of the porphyrin restructuring during the change in oxidation state. We previously demonstrated that the mutual interactions of the Fe(II)-porphyrin, its superstructure and the axial ligand rings can cause nonplanar distortions of the tetrapyrrole. The present investigation reveals that each Fe-porphyrin system adopts a specific redox transition in terms of energy and heme structure. Due to decreased ionic radii of the iron atom upon oxidation, an energetic adjustment occurs. The general trend is that the iron oxidation produces a deformation of the tetrapyrrole associated with a contraction of the porphyrin core and/or a shortening of the Fe$-$N(pyrrole) bonds. The important point is that the extent of this energetic fit is variable, depending on the superstructures around the Fe-macrocycle. In heme proteins, the heme restructuring upon iron oxidation is likely dependent on the amino acids surrounding the heme. These amino acids could play a role similar to that of the superstructures of FeBHP and FePFP.